High-Generation Polycationic Dendrimers Are Unusually Effective at Disrupting Anionic Vesicles: Membrane Bending Model

Zhi-Yi Zhang and Bradley D. Smith*

Department of Chemistry and Biochemistry, University of Notre Dame, Notre Dame, Indiana 46556. Received February 17, 2000; Revised Manuscript Received June 15, 2000

The membrane disruption properties of high generation (G4 to G7) poly(amidoamine) (PAMAM) dendrimers are evaluated and compared to linear poly(lysine). The G6 and G7 dendrimers are unusually effective at inducing leaky fusion of anionic, large unilamellar vesicles, as determined by standard fluorescence assays for lipid mixing, leakage, and contents mixing. Both G7 dendrimer and poly(lysine) are able to disrupt sterically stabilized vesicles that are coated with poly(ethylene glycol). A G7 dendrimer/DNA complex with a 1:1 concentration ratio of dendrimer surface amines to DNA phosphate groups is unable to induce leakage of 3:7 POPA-PE vesicles; however, extensive leakage is observed when the surface amine to phosphate stoichiometry is ≥3:1. Thus, the DNA/dendrimer complexes that typically induce high levels of cell transfection are also able to induce high levels of vesicle leakage. The G7 dendrimer does not induce membrane phase separation in 3:7 POPA-PE vesicles, but an inverse hexagonal phase is observed by ^{31}P NMR. The enhanced membrane disruption is interpreted in terms of a membrane bending model. A rigid, polycationic dendrimer sphere uses electrostatic forces to bend a malleable, anionic membrane and induce bilayer packing stresses. This bending model is biomimetic in the sense that protein-induced membrane bending is currently thought to be an important factor in the fusion mechanism of influenza virus.

INTRODUCTION

Dendritic polymers have a promising future as drug delivery vehicles (*1*, *2*) and as cell transfection agents (*3*−*14*). The hope is that dendrimers will enhance efficacy by improving delivery issues such as targeting, stability, and bioavailability. At present, the field is in its infancy, and the literature contains little discussion of how delivery is likely to occur at the molecular level. In particular, the current understanding of how dendrimers interact with bilayer membranes is quite weak. A major problem is the complexity and heterogeneity of the biomembrane matrix which makes it difficult to interpret results. Similarly, enhanced cell transfection has been reported using polydisperse mixtures of fractured dendrimers as DNA carriers (*3*); however, it is difficult to rationalize these results without knowing more about these complex delivery systems. In an effort to better understand the underlying supramolecular chemistry, we have chosen to study the interaction of monodisperse dendrimers with vesicle membranes.

This paper describes the effects that commercially available polycationic polyamidoamine (PAMAM)[1] dendrimers have on anionic unilamellar vesicles. The PAMAM dendrimers have an ethylenediamine core (Scheme 1) and are prepared by an iterative sequence of reactions (*2*). The number of surface amine groups doubles with each generation and the dendrimer diameter increases incrementally (Table 1). Generations 4 (G4) and below have open structures and ellipsoidal shapes, whereas G5 and above have closed-shell structures and are spherical (*2*, *15*). The goal of the study was to ascertain if PAMAM dendrimers interact with vesicle membranes in a size- or shape-dependent manner. We have evaluated the membrane disruption ability for dendrimer generations G4 to G7, and we find that, compared to linear poly(lysine), the higher generations are unusually effective at disrupting anionic vesicle membranes. A biomimetic membrane bending model is proposed to explain this observation.

EXPERIMENTAL PROCEDURES

All phospholipids including NBD-PE and Rh-PE were purchased from Avanti Polar Lipids. Py-PE, Py-C10-HPM, R18, ANTS, and DPX (Molecular Probes), poly(lysine) HBr salts (Sigma, polydispersity of 1.2), and 49KD-poly(glutamic) acid sodium salt (Sigma, polydispersity of 1.2) were purchased and used without further purification. The 4.7 kb pEGFP-N1 vector (Clontech) was propagated in *Escherichia coli* and purified using a QIAGEN tip and the associated QIAGEN protocol. Fluo-

* To whom correspondence should be addressed. Phone: (219) 631 8632. Fax: (219) 631 6652. E-mail: smith.115@nd.edu.

[1] Abbreviations: ANTS, 1-aminonaphthalene-3,6,8-trisulfonate; DMPC, 1,2-dimyristoyl-sn-glycero-3-phosphocholine; DPX, *N*,*N*′-*p*-xylenebis(pyridinium bromide); HPTS, 8-hydroxypyrene-1,3,6-trisulfonic acid; NBD-Taurine, *N*-(7-nitrobenz-2-oxa-1,3-diazol-4-yl)aminoethanesulfonic acid; LUVs, large unilamellar vesicles; NBD-PE, 1,2-dipalmitoyl-sn-glycero-3-phosphoethanolamine- *N*-(7-nitrobenz-2-oxa-1,3-diazol-4-yl); PAMAM, polyamidoamine; PE, phosphatidylethanolamine (egg); PEG, poly(ethylene glycol); PEG-2000-DOPE, 1,2-dioleoyl-sn-phosphatidylethanolamine-*N*-(poly(ethylene glycol)2000); POPA, 1-palmitoyl-2-oleoyl-sn-glycero-3-phosphatidic acid; POPC, 1-palmitoyl-2-oleoyl-sn-glycero-3-phosphocholine; POPS, 1-palmitoyl-2-oleoyl-sn-glycero-3-phosphoserine; PS, phosphatidylserine (bovine brain); Py-C10-HPM, 1-hexadecanoyl-2-(1-pyrenedecanoyl)-sn-glycero-3-phosphomethanol; Py-PE, 1-hexadecanoyl-2-(1-pyrenedecanoyl)-sn-glycero-3-phosphoethanolamine; R18, octadecyl rhodamine B chloride; Rh-PE, 1,2-dipalmitoyl-sn-glycero-3-phosphoethanolamine-*N*-(lissamine rhodamine B sulfonyl); SUVs, small unilamellar vesicles; TES, *N*-tris(hydroxymethyl)methyl-2-aminoethanesulfonic acid.

10.1021/bc000018z CCC: $19.00
Published on Web 09/19/2000

Scheme 1

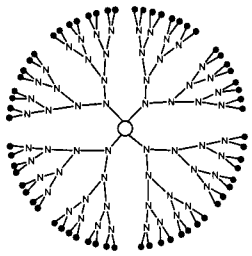

G4-PAMAM Dendrimer

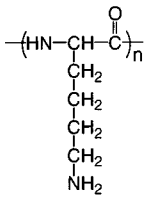

Poly(lysine)

○ = N-$(CH_2)_2$-N

N–N = N-$(CH_2)_2$-CO-NH-$(CH_2)_2$-N

N–● = N-$(CH_2)_2$-CO-NH-$(CH_2)_2$-NH_2

Table 1. Polymer Sizes

polymer	molecular weight	no. of surface amines	mean diameter (nm)
G4-PAMAM	14 215[a]	64[a]	
G5-PAMAM	28 826[a]	128[a]	4.3[c]
G6-PAMAM	58 048[a]	256[a]	6.9[c]
G7-PAMAM	116 493[a]	512[a]	8.0[c]
7.5K-poly(lysine)	7500[b]	36[b]	
34K-poly(lysine)	34 300[b]	164[b]	
100K-poly(lysine)	99 500[b]	476[b]	

[a] Theoretical value. [b] Average value, polydispersity around 1.2. [c] Experimental values reported in ref *15*.

rescence measurements were recorded on a Perkin-Elmer LS 50B instrument and all experiments were conducted at 25 °C.

PAMAM Dendrimers. The dendrimers were purchased from Dendritech. An ongoing concern in dendrimer science is sample purity. It is not straightforward to unambiguously establish the structural purity of high-generation dendrimers. The two most likely impurites are larger dendrimer−oligomers and smaller low-generation structures. A chromatographic analysis of the G7 dendrimers used in this study, conducted by the vendor, indicated that the sample was approximately 90% monodendrimer, 7% oligodendrimer, and 3% low-generation material. Thus, we cannot rule out the possibility that a fraction of the membrane disruption activity induced by the G7 dendrimer sample may be due to a small amount of highly active oligodendrimer impurity. However, even if this is true, the proposed model for dendrimer-induced membrane disruption would be essentially unchanged.

Vesicle Preparation. A solution of lipids in chloroform was evaporated using a rotary evaporator (<30 °C), and the resulting film was dried under vacuum for at least 1 h. The vesicles were dispersed in (1) 25 mM ANTS in 40 mM NaCl/5 mM TES (pH 7.4), (2) 90 mM DPX in 5 mM TES (pH 7.4), or (3) 12.5 mM ANTS/45 mM DPX/20 mM NaCl/5 mM TES (pH 7.4) with the aid of a Vortex mixer. Pyrex glass beads were added before vortexing to facilitate removal of the lipid film from the sides of the flask. The resulting opaque dispersion was frozen in an ethanol/dry ice bath and then allowed to thaw in a water bath at 35−40 °C. This freeze−thaw cycle was repeated 10 times. The resulting mixture was extruded, at room temperature, 29 times through a 19 mm polycarbonate filter (Nucleopore) typically with 100 nm diameter pores using a hand-held Basic LiposoFast device purchased from Avestin. The size of vesicles was routinely checked by dynamic light scattering using a Coulter N4 plus instrument. Separation of untrapped marker compound was achieved by dialysis (15 000 MW cutoff) against 150 mM NaCl.

Lipid Mixing Assays. Extents of lipid mixing were determined using three types of fluorescence probe dilution assays (*16*, *17*). The first two assays use anionic probes whereas the third uses a zwitterionic probe.

NBD-PE/Rh-PE Assay. One population of vesicles contained the probes NBD-PE and Rh-PE (0.6% each), whereas another population was unlabeled. Excitation was set at 470 nm and fluorescence emission was measured at 530 nm using a 515 nm filter. Labeled vesicles were mixed with an equal population of unlabeled vesicles (final lipid concentration was 50 μM) in 3 mL, pH 7.4, of buffer (100 mM NaCl/5 mM TES). Lipid mixing results in an increase in NBD-PE fluorescence intensity due to diminished quenching as the two probes are diluted. The residual fluorescence was taken as 0% lipid mixing, and 100% mixing was set using vesicles containing 0.3% of the probes. Control experiments showed that NBD-PE fluorescence is not affected by interactions with the polycations. For example, addition of polycations to solutions of probe-containing vesicles that had been disrupted with Triton X-100 produced no change in fluorescence.

R18 Assay. Excitation was set at 560 nm and fluorescence emission was measured at 590 nm. The 2% R18 labeled vesicles (5 μM) were mixed with unlabeled vesicles (45 μM) in 3 mL of 100 mM NaCl/5 mM TES (pH 7.4) buffer. The initial fluorescence was taken as 0% lipid mixing and 100% mixing was determined by addition of Triton X-100 to give 0.5%(w/v).

Py-PE assay. Excitation was set at 320 nm and fluorescence emission was measured at 395 and 470 nm. The ratio of I_{470nm}(ex) to I_{395nm}(mon) was determined as a function of time. The 5% labeled vesicles (5 μM) were mixed with unlabeled vesicles (45 μM) in 3 mL of 100 mM NaCl/5 mM TES (pH 7.4) buffer. Vesicles (50 μM) containing 0.5% of Py-PE were used to calibrate the ratio of I_{470nm}(ex)/I_{395nm}(mon) corresponding to 100% lipid mixing.

Leakage Assay. The fluorophore ANTS and its collisional quencher DPX were co-encapsulated in a single population of vesicles. Leakage results in an increase in ANTS fluorescence intensity due to dimished quenching as the two probes are diluted (*17*). Control experiments established that both dendrimer and poly(lysine) slightly enhance the fluorescence of ANTS but the presence of excess poly(glutamate) restores the original fluorescence intensity. Excitation was set at 355 nm and fluorescence emission was measured at 530 nm using a 515 nm filter. At $t = 0$ s, vesicles (50 μM lipid) containing ANTS/DPX were dispersed in 3 mL of 100 mM NaCl/5 mM TES (pH 7.4) buffer, and the residual fluorescence was taken as 0% leakage. At $t = 100$ s, the system was treated with polycation, and at $t = 300$ s, poly(glutamate) was added to eliminate extraneous signal due to polycation/ANTS interaction. The fluorescence intensity corresponding to 100% leakage was determined by addition of 0.3% (w/v) Triton X-100.

Contents Mixing Assay. Attempts to measure aqueous contents mixing using the Tb^{3+}/DPA asssay (*17*) were unsuccessful due to light scattering problems. The use of sodium inositol hexaphosphate as a vesicle deaggregation agent was not helpful in our hands (*18*). The calcein/Co^{2+} assay (*19*) could not be employed due to precipitation of a dendrimer/Co^{2+} complex. A problem with the ANTS/DPX assay (*17*) was enhancement of leaked ANTS fluorescence upon interaction with the

dendrimer; however, the presence of excess poly(glutamate) reverses the polycation/ANTS interaction and restores the original ANTS emission spectrum. At $t = 0$ s, vesicles containing ANTS were mixed in 3 mL of 100 mM NaCl/5 mM TES (pH 7.4) buffer with an equal concentration of vesicles containing DPX (final lipid concentration was 50 μM). At $t = 100$ s, the system was treated with polycation, and at $t = 300$ s, poly(glutamate) was added. The initial fluorescence was taken as 0% contents mixing, and a solution of ANTS/DPX-containing vesicles (50 μM) in 3 mL of 100 mM NaCl/5 mM TES (pH 7.4) buffer was used for the calibration of 100% contents mixing.

^{31}P NMR. Aqueous lipid dispersions were prepared by vortexing 50 mM POPA/PE (3:7) in 1.0 mL of an aqueous buffer (100 mM NaCl, 5 mM TES, pH 7.4) and then adding of G7-PAMAM dendrimer or 100K-poly(lysine) (10 mM of surface amines). Prior to the NMR measurements, 0.1 mL of D_2O was introduced into the samples. The ^{31}P NMR spectra (121 MHz) were acquired at 25 °C using a phase-cycled Hahn spin−echo sequence (*20*). In each case, about 1000 scans were collected with a recycling delay of 3 s and line broadening of 100 Hz. The chemical shifts are relative to small phosphatidylcholine vesicles at 0 ppm.

Dendrimer Internalization Assays. Three different methods were used to detect dendrimer entry into 3:7 POPA/PE vesicles.

HPTS/DPX Assay (21). A dispersion (311 μL) of G7-PAMAM, the water-soluble anionic dye HPTS, and 3:7 POPA/PE vesicles (200 nm) was incubated for 200 s at 25 °C and then added to a gently stirred solution of 40 mM DPX (2689 μL) (final concentrations: G7-PAMAM surface amine 10 μM, HPTS 1.0 μM, and phospholipids 1.0 mM). The intensity of the HPTS emission at 510 nm was measured using the pH-independent excitation wavelength of 413 nm (I). In a separate experiment, the HPTS intensity was measured for a sample that contained water instead of 40 mM DPX (I_{100}). Finally, aqueous Triton X-100 was added (0.5% w/v) to the DPX containing sample and the intensity of the HPTS emission at 413 nm was remeasured (I_0). The percentage of internalized HPTS was calculated as $(I - I_0)/(I_{100} - I_0) \times 100\%$.

NBD-Taurine Assay. To a mixture of G7-PAMAM (5 μM of surface amine) and NBD-taurine (0.5 μM) in 3 mL of buffer (100 mM NaCl, 5 mM TES, pH 7.4) were added 3:7 POPA/PE vesicles (50 μM; 100, 200, or 400 nm). After incubation at 25 °C for 200 s, the dispersion was treated with poly(glutamate) (250 μM of surface carboxylate), and then 200 s later, the intensity of the NBD-taurine emission at 530 nm using excitation wavelength of 470 nm was measured (I_{100}). Sodium dithionite (30 mM) was added and the NBD-taurine emission was measured after 10 min (I). Finally, aqueous Triton X-100 was added (0.5% w/v) and the NBD-taurine emission was measured (I_0). The percentage of internalized NBD-taurine was calculated as $(I - I_0)/(I_{100} - I_0) \times 100\%$.

NBD-G7 Assay. An NBD−dendrimer conjugate (10% NBD−G7) with 10% of the surface dendrimer amines labeled with NBD was prepared by stirring a mixture of G7-PAMAM (9.1 mg, 40 μmol surface amine) and 7-nitrobenz-2-oxa-1,3-diazol-4-chloride (NBD-Cl, 0.8 mg, 4.0 μmol) in methanol (500 μL) in the dark at room temperature for 18 h. TLC (silica gel/chloroform) indicated that the NBD-Cl was consumed. The solvent was evaporated to give a yellow solid which was used without purification. To a solution of 10% NBD−G7 (10 μM of surface amine) in 3 mL of buffer (100 mM NaCl, 5 mM TES, pH 7.4) was added 3:7 POPA/PE vesicles (200 nm, 1.0 mM). After incubation at 25 °C for 200 s, the intensity of the 10% NBD−G7 emission at 530 nm was measured using excitation wavelength of 470 nm (I_{100}). Sodium dithionite (30 mM) was added and the emission was measured after 10 min (I). Finally, aqueous Triton X-100 was added (0.5% w/v) and the 10% NBD−G7 emission was measured (I_0). The percentage of internalized 10% NBD−G7 was calculated as $(I - I_0)/(I_{100} - I_0) \times 100\%$.

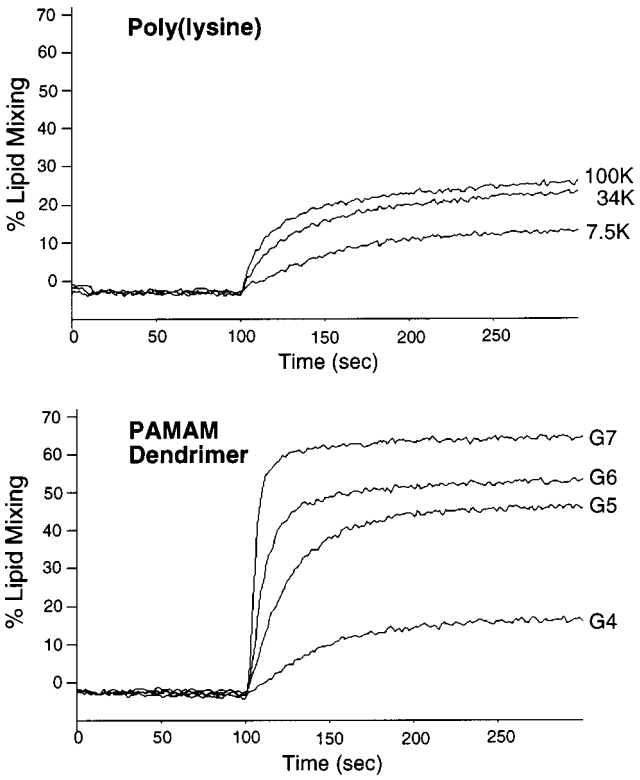

Figure 1. Lipid mixing of 3:7 POPA/PE vesicles at pH 7.4 and 25 °C. A population of vesicles containing NBD-PE/Rh-PE was mixed with an equal amount of unlabeled vesicles (final [phospholipid] = 50 μM), and treated with polycation at $t = 100$ s. In each case, the concentration of polymer surface amines was 10 μM.

RESULTS

Lipid Mixing. The polycation-induced intermixing of lipid bilayers was monitored using three different fluorescence probe dilution assays (*16, 17*) Generally, the resonance energy transfer pair of NBD-PE and Rh-PE was employed. Since these probes are anionic and the fusogens are polycationic, it was important to eliminate the possibility of artifacts due to probe transfer, phase separation, and probe/polycation interaction. Therefore, a number of the lipid-mixing experiments were repeated using the R18 probe or the zwitterionic Py-PE. In essentially all cases, the lipid mixing results were found to be probe independent.

The first vesicles examined were anionic, large unilamellar vesicles (LUVs, 100 nm diameter) composed of 3:7 POPA/PE. Two equal populations of 3:7 POPA/PE vesicles were mixed at $t = 0$ s (final concentration of phospholipid was 50 μM). One population contained the NBD-PE and Rh-PE, whereas the other was unlabeled. An aliquot of polymer was added at $t = 100$ s, to give a final concentration of polymer surface amines of 10 μM. As shown in Figure 1 and Table 2 (entry 1), the extent of lipid mixing increased only slightly with the molecular weight of poly(lysine), but increased markedly with dendrimer molec-

Table 2. Extents (%) of Lipid Mixing, Leakage, and Contents Mixing[a]

entry	assay	vesicle composition	G4 PAMAM	G5 PAMAM	G6 PAMAM	G7 PAMAM	7.5K poly(lysine)	34K poly(lysine)	100K poly(lysine)
1	lipid mixing	POPA-PE 3:7	16[b]	46[b]	53	64	13[b]	24	26
2	lipid mixing	POPS-PE 3:7				45			10
3	lipid mixing	POPA-POPC 3:7	c	c	c	2	0	c	c
4	lipid mixing	PS-POPC 3:7	c	c	c	0	c	c	c
5	lipid mixing	POPA-POPC 4:1	b	0	7	25	3	11	14
6	lipid mixing	PS-POPC 4:1	0	4	7	20	0		0
7	lipid mixing	PS	c	c	c	18	c	c	0
8	leakage	POPA-PE 3:7	5[b]	6	37	58	4	4	4
9	contents mixing	POPA-PE 3:7	11[b]	6	6	4	19	12	12

[a] 100 nm unilamellar vesicles, total lipid concentration = 50 μM, concentration of polymer surface amines = 10 μM. [b] Precipitation occurred after measurement. [c] Rapid precipitation obscured measurement.

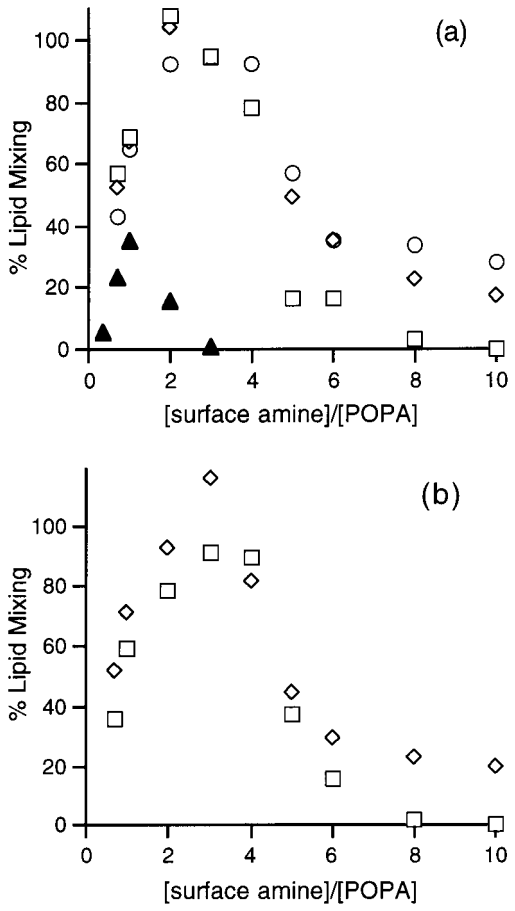

Figure 2. Lipid mixing as a function of the concentration ratio of polymer surface amines to POPA (100 nm, [phospholipid] = 50 μM, pH 7.4, 25 °C) (a) 3:7 POPA/PE vesicles: (▲) 100K-poly-(lysine), NBD-Rh assay; (◇) G7-PAMAM, NBD-Rh assay; (○) G7-PAMAM, Py-PE assay; (□) G7-PAMAM, R18 assay. (b) 3:7 POPA/PE vesicles containing 2% PEG-2000-DOPE: (◇) G7-PAMAM, NBD-Rh assay; (□) G7-PAMAM, R18 assay. Uncertainty ± 5% units.

ular weight. Furthermore, a high-generation dendrimer was more effective than a poly(lysine) with a similar number of surface amines. When excess poly(glutamate), a strong binder of polycations (*22*), was added to the vesicles before the polymer, no lipid mixing occurred, indicating that electrostatic interactions are driving vesicle aggregation and the subsequent lipid mixing.

The effect of polycation concentration on lipid mixing was examined using G7 dendrimer and 100K-poly-(lysine). As shown in Figure 2a, the general trend is the same for both polycations; that is, the extent of lipid mixing of 3:7 POPA/PE vesicles initially increases with concentration, reaches a maximum, and then decreases (*18*, *23*, *24*) At low concentrations, the polycations cross-link and aggregate the anionic vesicles, but at higher concentrations the polycations coat the vesicles and hinder close approach. In the case of poly(lysine), lipid mixing was a maximum when the concentration ratio of surface amine to POPA was 1, an observation that has been noted before (*23*). In the case of G7 dendrimer, lipid mixing was maximal when the ratio of surface amine to POPA was about 3. The higher charge ratio is likely due to the rigid and spherical structure of the dendrimer which can only contact a vesicle with a fraction of its available surface amines. Thus, a higher concentration of surface amines is needed to reach the optimal level of cross-linking and charge neutralization.

The results of vesicle composition studies are summarized in Table 2 (entries 1−7). When the fusion inhibitor POPC (*18*, *25*) was used instead of PE, almost no lipid mixing was observed with G7 dendrimer (compare entries 1 and 3). However, significant lipid mixing occurred when the fraction of POPA was increased (compare entries 3 and 5). Interestingly, there was little or no lipid mixing induced by 100K-poly(lysine) when PS was used instead of POPA (compare entries 1 and 2 and 5 and 6) or even when the LUVs were composed of 100% PS (entry 7). This observation is in agreement with a previous study using LUVs (*18*), but contrasts with a report that poly(lysine) is able to fuse SUVs containing PS (*23*).

As summarized in Table 3, the presence of 2% PEG-2000-DOPE in 3:7 POPA/PE vesicles greatly decreases the extent of lipid mixing induced by $CaCl_2$ (entry 10). In this case, aggregation of the sterically hindered vesicles, a requisite step for fusion, is greatly inhibited (*26*). In contrast, both G7-PAMAM dendrimer (entries 12 and 13) and 100K-poly(lysine) (entries 14 and 15) are still able to induce the sterically stabilized vesicles to undergo significant amounts of lipid mixing. A study of lipid mixing as a function of G7 dendrimer concentration resulted in a bell-shaped profile that closely matches that seen with conventional 3:7 POPA/PE vesicles (Figure 2).

The effect of added NaCl on polycation-induced lipid mixing of 3:7 POPA/PE vesicles is summarized in Table 4. Surprisingly, the extent of lipid mixing increases with increasing NaCl concentration. This relationship is the reverse to that observed with Ca^{2+}-mediated fusion (*27*).

Leakage. Leakage was measured using the ANTS/DPX fluorescence assay (*17*) As shown in Figure 3 and Table 2 (entry 8), low and high molecular weight poly-(lysine) induced very little leakage. The same result was obtained with the low-generation dendrimers but the G6 and G7 dendrimers induced rapid and drastic leakage. When excess poly(glutamate) was added before the polycations no leakage occurred. Leakage from conventional and sterically stabilized 3:7 POPA/PE vesicles was

Table 3. Extents (%) of Cation-Induced Lipid Mixing of Conventional and Sterically Hindered Vesicles[a]

entry	assay	cation	charge ratio (±)[b]	conventional (3:7, POPA/PE)[a]	sterically hindered[a]
10	R18	$CaCl_2$ (1 mM)		86	7
11	NBD-PE Rh-PE	$CaCl_2$ (20 mM)			6
12	R18	G7 PAMAM	1:1	69	59
13	NBD-PE Rh-PE	G7 PAMAM	1:1	83	71
14	R18	100K poly(lysine)	1:1	39	15
15	NBD-PE Rh-PE	100K poly(lysine)	1:1	41	35

[a] Conventional vesicles were 3:7 POPA/PE (100 nm, 50 μM phospholipid, pH 7.4, 25 °C). Sterically hindered vesicles contained an additional 2% PEG-2000-DOPE, lipid mixing uncertainty ± 5%. [b] Concentration ratio of polycation surface amines to POPA.

Table 4. Effect of NaCl Concentration on Extent (%) of Polycation-Induced Lipid Mixing of 3:7, POPA/PE Vesicles[a]

[NaCl] (mM)	G7 PAMAM[b]	100K poly(lysine)[b]
100	56	34
200	78	35
300	74	33
400	78	42
500	67	41

[a] [phospholipid] = 50 μM, 5 mM TES buffer, pH 7.4, 25 °C, lipid mixing uncertainty ± 5%. [b] Concentration ratio of polycation surface amines to POPA was 2:3.

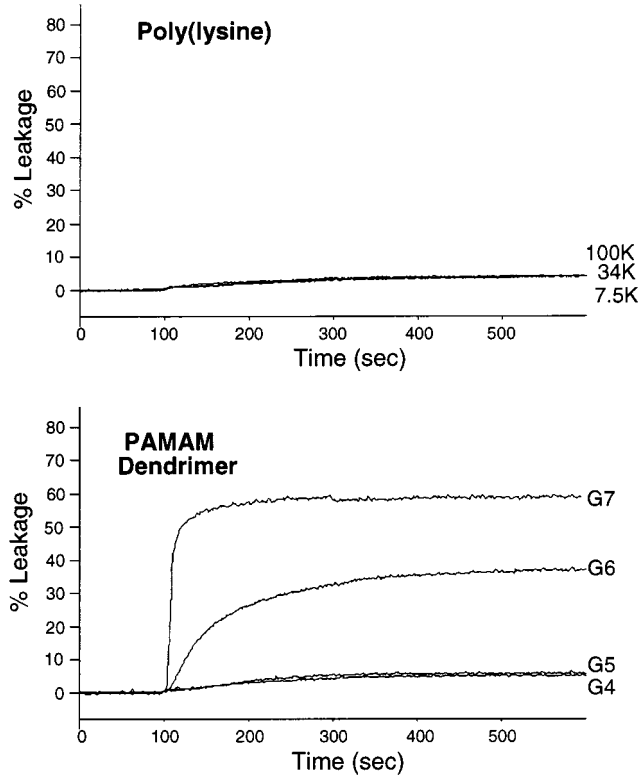

Figure 3. Leakage from 3:7 POPA/PE vesicles (100 nm, [phospholipid] = 50 μM, pH 7.4, 25 °C) containing ANTS/DPX. The vesicles were treated with polymer at t = 100 s (in each case, the concentration of polymer surface amines was adjusted to 10 μM), and with poly(glutamate) (500 μM carboxylates) at t = 300 s.

monitored as a function of G7-PAMAM concentration. As shown in Figure 4, both systems exhibit bell-shaped dependencies that are very similar to the lipid mixing profiles in Figure 2.

The leakage of ANTS/DPX from 3:7 POPA/PE vesicles at pH 7.4 (100 mM NaCl/5 mM TES) and 25 °C induced by complexes of DNA and G7 dendrimer is shown in Figure 5. DNA (pEGFP-N1 vector, 4.7 kb, the plasmid codes for enhanced green fluorescent protein and is commonly used to measure cell transfection efficiency)

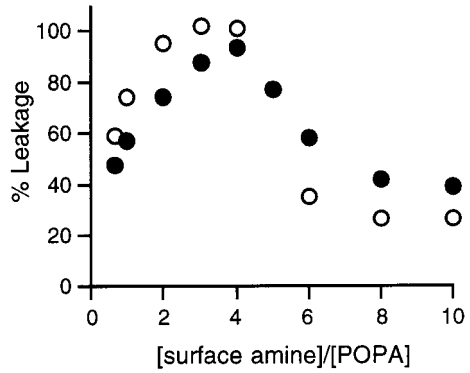

Figure 4. Leakage as a function of the concentration ratio of G7-PAMAM surface amines to POPA (pH 7.4, 25 °C); (○) 3:7 POPA/PE vesicles (100 nm, [phospholipid] = 50 μM); (●) sterically hindered 3:7 POPA/PE vesicles containing 2% PEG-2000-DOPE. Uncertainty ± 5%age units.

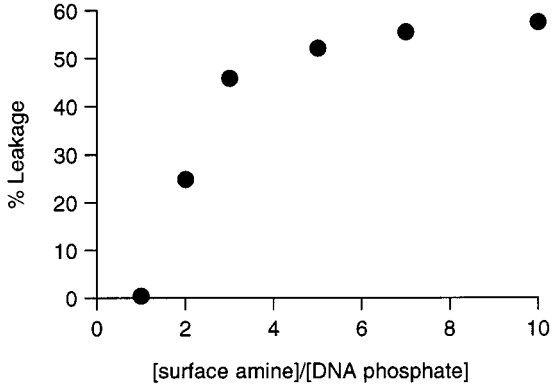

Figure 5. Leakage from 3:7 POPA/PE vesicles (100 nm, 50 μM lipid, pH 7.4, 25 °C) containing ANTS/DPX, induced by G7 dendrimer/DNA complexes at different concentration ratios of dendrimer surface amine to DNA phosphate groups. In each case, the concentration of G7 dendrimer surface amines was 10 μM.

and G7 dendrimer were mixed at different concentration ratios of dendrimer surface amine to DNA phosphate group. After 5 min, the dendrimer/DNA complexes were added to the vesicles (50 μM phospholipid) at pH 7.4 (100 mM NaCl/5 mM TES). In each case, the final concentration of G7 dendrimer surface amines was 10 μM. No leakage was observed when the surface amine/DNA phosphate ratio was unity, whereas the leakage induced by a surface amine/DNA phosphate ratio of 3:1 was 80% of the extensive leakage induced by G7 dendrimer alone. Previous work has shown that monodisperse particles are formed when the surface amine/DNA phosphate ratio is 3:1, with diameters around 100 nm and ζ-potentials of +50 mV (*28*−*30*).

Contents Mixing. The amount of contents mixing of 3:7 POPA/PE vesicles, determined using the ANTS/DPX assay (*17*), is summarized in Table 2 (entry 9). Poly(lysine) induced a modest amount of contents mixing at

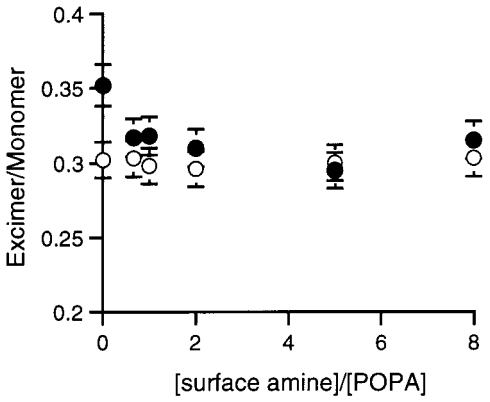

Figure 6. Excimer/monomer ratio as a function of the concentration ratio of G7-PAMAM surface amines to POPA (3:7 POPA/PE vesicles, 100 nm, 50 μM phospholipid, pH 7.4, 25 °C); (○) Py-PE; (●) Py-C10-HPM.

about the same rate as lipid mixing (see Figure 1). Very little contents mixing was observed with G6 and G7 dendrimers because leakage was so rapid and extensive.

Membrane Fluidity. Pyrene-containing lipids are used as probes to detect lateral phase separation and changes in membrane fluidity (*31*, *32*). Polycations have been shown to induce phase separation in certain anionic membranes, which is reflected by an increase in the pyrene excimer/monomer ratio (*31*), whereas in other cases, an observed decrease in excimer/monomer ratio has been interpreted as a decrease in the rate of lateral diffusion (*31*, *32*). Two pyrene-containing probes were used in this study, zwitterionic Py-PE and anionic Py-C10-HPM. Addition of increasing amounts of G7 dendrimer to 3:7 POPA/PE vesicles containing 5% Py-PE (50 μM lipid, pH 7.4) resulted in no detectable change in the excimer/monomer ratio (Figure 6). Addition of increasing amounts of G7 dendrimer to 3:7 POPA/PE vesicles (50 μM lipid, pH 7.4) containing 5% Py-C10-HPM produced a U-shaped dependence, with an initial decrease in the excimer/monomer ratio followed by a subsequent increase (Figure 6). The data indicates that G7 dendrimer does not induce phase separation in 3:7 POPA/PE vesicles, does not effect the lateral diffusion of the zwitterionic PE, but does slow the diffusion of the anionic POPA. The U-shaped dependence on excimer/monomer ratio has been noted before (*31*−*33*) and is attributed to the gradual delocalization of positive sites as the membrane surface becomes saturated with polycation.

^{31}P NMR spectroscopy. ^{31}P NMR line shapes are often used to identify changes in membrane morphologies (*34*). For example, ^{31}P NMR was employed in conjuction with freeze−fracture techniques to show that the near-spherical polycationic protein, cytochrome *c*, induces anionic cardiolipin-containing membranes to undergo a phase change from bilayer to inverse hexagonal, H_{II} (*35*). In contrast, linear poly(lysine) does not induce such a morphology change to inverse membrane curvature (*36*). A similar result is seen in Figure 7, which shows the change in ^{31}P NMR line shapes upon treatment of 3:7 POPA/PE vesicles (50 mM lipid, pH 7.4, 5 mM TES, 100 NaCl) with polycation. In the absence of polycation the typical bilayer pattern is observed (Figure 7A). Addition of poly(lysine) (10 mM of surface amines) results in precipitation with no major change in line shape (Figure 7B). Addition of G7-PAMAM dendrimer (10 mM of surface amines) also produces a precipitate, but there is concomitant formation of hexagonal II phase as reflected by the reduced line width and the characteristic reverse peak asymmetry (Figure 7C) (*34*, *35*)

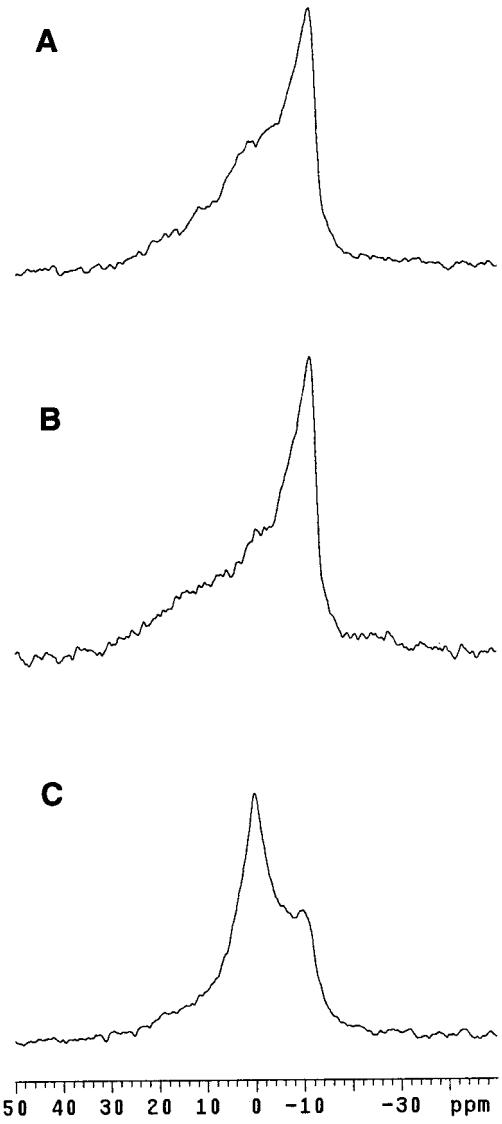

Figure 7. ^{31}P NMR spectra of 3:7, POPA/PE vesicles (50 mM phospholipid) in 5 mM TES, 100 mM NaCl, pH 7.4, 25 °C. (A) no addition, (B) addition of 100K-poly(lysine) (10 mM surface amines), (C) addition of G7-PAMAM dendrimer (10 mM surface amines).

No Dendrimer Internalization. Three related assays were used to determine if the G7-PAMAM dendrimers were internalized by 3:7 POPA/PE vesicles at pH 7.4. The first method was recently described by Tedesco and Matile (*21*). Vesicles (3:7 POPA/PE, 200 nm) were treated with dendrimer (at low surface amine to POPA) and the anionic fluorescent dye HPTS. If the dendrimers entered the vesicle by an endovesiculation mechanism, then presumably some HPTS should also be internalized at the same time. The internalized HPTS can be detected because it is protected from the externally added quencher DPX (*21*). The second method employed the anionic water soluble dye NBd-taurine as a replacement for HPTS and used externally added sodium dithionite as a chemical quencher of the NBD-taurine (*37*) Both methods were unable to produce evidence for internalization of the anionic dyes. A third method resorted to covalent attachment of the NBD dye to the PAMAM dendrimer. A dendrimer−NBD conjugate (10% NBD−G7) was prepared with 10% of the surface dendrimer amines labeled with NBD. Incubation of the 10% NBD−G7 conjugate with excess 3:7 POPA/PE vesicles, and subsequent chemical quenching by dithionite again showed no evi-

dence for internalization of the NBD−G7 conjugate. We conclude that the dendrimers are not internalized into a protective environment within the vesicles, although the results do not rule out the possibility that dendrimers enter the vesicles but remain accessible to the quenching probes.

DISCUSSION

Membrane Disruption Using Poly(Lysine). Peptidyl polycations such as poly(lysine) are well-known to bind tightly to anionic vesicles [each basic residue contributes about 1 kcal/mol to the membrane binding energy (*38*, *39*)] and promote vesicle−vesicle interaction. The specific outcome (aggregation, leakage, lipid mixing, contents mixing) depends on the composition and size of the vesicles. For example, poly(lysine) promotes the aggregation and complete fusion of anionic SUVs (*23*, *40*), whereas treatment of LUVs with poly(lysine) usually results in hemifusion, i.e., lipid mixing only and no mixing of aqueous contents (*18*, *41*). The increased fusogenicity of SUVs is attributed to the greater membrane curvature strain (*42*).

During the course of this study we confirmed a previous report (*18*) that poly(lysine) is able to promote the lipid mixing of PA-containing LUVs more effectively than PS-containing LUVs (entries 1, 2, 5−7, Table 2). This may be due to the different structures that poly(lysine) forms on the membrane surfaces. It is well-established that poly(lysine) is a random coil in neutral solution, but adopts a β-sheet on a PA membrane surface (*43*−*45*), and forms α-helices on a PS membrane surface (*46*). The same conformations but with reduced content are also observed in mixed PA−PC (*47*) and PS−PC (*46*) vesicles. In addition, there is evidence that poly(lysine) induces significant lateral phase separation in PA−PC vesicles (*44*, *45*, *48*) but not so in PS−PC (*46*) or PS−PE vesicles (*32*). Thus, poly(lysine) β-sheets on a PA surface appear to induce more lipid mixing than α-helices on a PS surface. The β-sheet structures may force a closer approach of apposed dehydrated surfaces, and/or increase the number of surface defects due to lateral phase separation (*49*).

Membrane Disruption Using PAMAM Dendrimers. High-generation PAMAM dendrimers are unusually effective at disrupting anionic vesicles. Specifically, G6 and G7 dendrimers rapidly induce large amounts of lipid mixing and leakage of aqueous contents (Figures 1 and 3). They are much more effective than low-generation PAMAM dendrimers or poly(lysine) of any molecular weight, even when the polymer concentrations are adjusted so that the number of exposed surface amines is constant. For example, G7 dendrimer (20 nM of polymer) induces four times more lipid mixing and twelve times more leakage in 3:7 POPA-PE vesicles (50 μM total lipid) than an 8-fold higher concentration of G4 dendrimer (160 nM of polymer).

Both G7-PAMAM and 100K-poly(lysine) are able to disrupt sterically hindered, PEG-containing vesicles that are otherwise resistant to Ca^{2+}-induced fusion (Table 3, Figure 2, and Figure 4). Apparently, the polycations are able to overcome the surface hydration barrier provided by the external PEG chains and force the apposed membranes to undergo lipid mixing. Similarly, Ca^{2+}-mediated fusion is strongly inhibited by increasing NaCl concentrations (*27*), but the lipid mixing induced by PAMAM dendrimers and poly(lysine) actually increases with NaCl concentration (Table 4). Na^+ ions are thought to affect fusion in opposing ways (*50*). They can associate with the anionic bilayer surface and promote lipid mixing because of charge neutralization. Conversely, they can inhibit vesicle aggregation by increasing the thickness of the repulsive hydration layer at the membrane surface (*50*). It appears that even in the presence of high NaCl concentrations, 100K-poly(lysine) and especially G7-PAMAM dendrimer are still able to cross-link the vesicles (*38*, *39*) and, because of increased charge neutralization, induce enhanced lipid mixing.

In general, the best cell transfection results with PAMAM dendrimers are observed with high-generation homologues and when the ratio of dendrimer surface amines to DNA phosphate groups is greater than unity (*3*−*14*, *29*). The dendrimer/DNA complexes formed under these conditions are irregular polycationic aggregates (*29*, *51*). We find that a G7 dendrimer/DNA complex with a 1:1 concentration ratio of dendrimer surface amines to DNA phosphate groups is unable to induce leakage of 3:7 POPA-PE vesicles; however, extensive leakage is observed when the surface amine to phosphate stoichiometry is $\geq$3:1 (Figure 5). Thus, the polycationic DNA/dendrimer complexes that typically induce high levels of cell transfection also induce the highest levels of vesicle leakage. The dendrimer/vesicle interaction is strongly dependent on the vesicle membrane composition. The polycationic dendrimers disrupt different types of anionic vesicles, especially PE-containing vesicles (Table 2). They do not disrupt zwitterionic PC vesicles (*52*, *53*) or anionic vesicles containing a high fraction of PC (Table 2). This membrane selectivity may explain some of the differences in transfection efficiencies and cell toxicities observed with different cell lines (*3*−*14*).[2]

Membrane Bending Model. Why are the higher generation dendrimers better at disrupting anionic membranes? Although a definitive answer cannot be provided at this time, it is worth emphasizing that high-generation PAMAM dendrimers are monomolecular weight polycations with spherical shapes of known diameters (Table 1) and that these structural attributes greatly simplify any analysis of their supramolecular properties. What can be stated with some certainty is that the observed membrane disruption is not due to a simple detergent effect. PAMAM dendrimers are highly water-soluble polycations [essentially all of the surface amine groups are protonated at neutral pH (*54*)]. The outer surface of a high-generation PAMAM dendrimer is highly congested and unlikely to be deeply penetrated by a phospholipid (*2*, *15*, *55*, *56*). Recent EPR studies show that there is very little interaction between G2-PAMAM dendrimers and zwitterionic DMPC vesicles (*52*). A modest interaction is observed with G7 dendrimers which leads to a partially perturbed bilayer structure, but the integrity of the membrane is preserved (*52*).

With anionic vesicles, the interaction is an electrostatic attraction between a malleable, anionic bilayer membrane (radius of curvature $\sim$50 nm), and a rigid, cationic dendrimer sphere (radius of curvature $\sim$4 nm). This leads to dendrimer-induced membrane bending as shown in Figure 8. When a polycationic dendrimer binds to the

[2] The vesicle disruption events reported in this paper are much faster than the process of cell transfection which occurs over a period of hours. However, it should be noted that the vesicles were typically composed of POPA/PE, an unnatural vesicle composition that was used specifically because of its relative instability and the expectation that the vesicles would magnify any disruption effect. At present it is not known if high generation PAMAM dendrimers have a special ability to disrupt biological membranes.

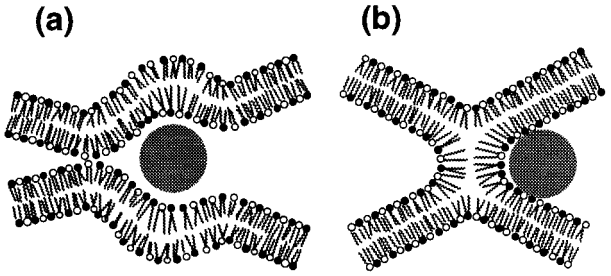

Figure 8. Schematic representation of dendrimer-induced bending of bilayer membranes. Lipids with black headgroups represent anionic phospholipids, the others may be zwitterionic phospholipids. (a) Cross section of a polycationic dendrimer that cross-links the exterior surfaces of two anionic vesicles. Electrostatic forces bend the bilayer surfaces and induce local regions of inverse curvature. (b) Cross-section of a polycationic dendrimer bound to two hemifused vesicles at the periphery of the vesicle-vesicle contact point.

exterior of an anionic vesicle, electrostatic forces bend the bilayer surface (*57*), and induce a local region of inverse curvature (*58*), which in turn induces packing stresses (*59*). If a dendrimer is situated at the connection point of two or more vesicles (Figure 8a) then the packing stresses lead to enhanced lipid mixing. Lipid mixing at a contact point on one side of the dendrimer produces the hemifused intermediate shown in Figure 8b. The structure has inversely curved surfaces at the periphery of the vesicle−vesicle contact point (*57*−*60*). We propose that high-generation polycationic dendrimers facilitate lipid mixing by electrostatically stabilizing these inversely curved, anionic surfaces (Figure 8b).[3] The crucial structural factors are the dendrimer's polycationic charge, rigid spherical shape, and highly congested exterior surface. The following observations support this hypothesis. (i) The vesicle disruption effect is specific for high-generation PAMAM dendrimers and is diminished with low-generation dendrimers or linear poly(lysine) of any molecular weight. (ii) Vesicle disruption is greatly diminished when POPC is used instead of PE (Table 2, compare entries 1−4). The PC headgroup is larger and more heavily hydrated than the PE headgroup (*58*) and it is energetically more costly for bilayers containing PC to adopt inverse curvature (*18*, *57*−*60*). (iii) ^{31}P NMR (Figure 7) shows that G7 dendrimer acts like the near-spherical polycationic protein, cytochrome *c* (*35*), and induces bilayer membranes to adopt an inverse hexagonal II phase. Linear poly(lysine) does not induce such a change to inverse curvature. (iv) The area per surface amine for PAMAM dendrimers decreases with each generation, and by G7 is about 70 Å^2/surface amine (see Figure 37 in ref *2*) which is close to the headgroup area for a typical fluid-phase bilayer membrane. Thus, the matched spacing between surface groups may lead to optimal charge neutralization and optimal membrane bending strain. (v) The dendrimer-induced membrane bending model is biomimetic in the sense that protein-induced membrane bending is thought to be an important factor in the fusion mechanism of Influenza virus (*62*, *63*).

[3] The hemifused intermediate shown in Figure 8b is often referred to as a stalk, and is an intermediate in the stalk fusion mechanism. However, the stalk hypothesis describes the fusion of uncharged membranes where electrostatic effects are minimal. Thus, this study of anionic membranes is not a test of the stalk hypothesis, but it does raise the possibility that some biological fusion systems may operate by a mechanism that is similar to that described in Figure 8b (*61*).

In addition to membrane bending, other factors may be contributing to the dendrimer's enhanced vesicle disruption ability. One possibility is lateral phase separation, which is thought to be an important factor in Ca^{2+}-mediated fusion (*50*). Polycations have been shown to induce phase separation in a number of anionic membrane compositions (*33*, *44*, *45*, *48*, *64*) but not so in others (*32*, *46*). We are unable to detect dendrimer-induced phase separation in 3:7 POPA/PE vesicles (Figure 6), but we cannot rule out transient microdomains. Another factor that cannot be discounted at present is an interaction between the dendrimer and the membrane surface. Poly(lysine) is thought to be situated above the polar headgroup region of the membrane, with perhaps a water monolayer between (*38*, *39*, *65*). An unusual structural feature with high generation PAMAM dendrimers is the densely packed spherical surface, which may not be properly hydrated for steric reasons. Thus, the dendrimers may possess an unusual ability to interact with, or dehydrate, the polar headgroups at the bilayer surface which may lead to enhanced fusion.

Drug Delivery and Cell Transfection. The membrane bending model suggests that dendrimers may be useful as fusion catalysts. Indeed, a polycationic G9 dendrimer was recently shown to dramatically enhance the fusion of reteroviral-infected murine cells (*66*). Thus, it may be possible to use dendrimers to improve vesicle-mediated drug delivery. The dendrimers could promote vesicle−cell fusion which would allow vesicle-encapsulated drugs to enter the cell.

As drug delivery vehicles, dendrimers can be viewed as either endo receptors with the drugs encapsulated in the dendrimer internal cavities (*1*, *2*, *56*) or they can be used as exo receptors with drugs bound to the dendrimer surfaces. An example of the latter approach is cell transfection. The recent commercial availability of PAMAM dendrimers has led to their increased use as cell transfection agents (*3*−*13*). Cell transfection is a complicated multistep process, but in many cases, it appears that transfection is mediated by endocytosis, and there is evidence that exit from the endosome is the step that controls transfection efficiency (*28*). Our results show that high generation PAMAM dendrimers have an unusual ability to disrupt bilayer membranes, which suggests that they may be able to permeate from endosomes. We tested this idea by trying to detect dendrimer entry into vesicles. Our lack of success does not necessarily mean that PAMAM dendrimers cannot pass through endosomal membranes.[2] It may be that the outward curvature of the vesicles prevents dendrimer influx. In the case of endosomal exit, the transport process is efflux which should be more favorable because the membrane curvature is reversed. Nonetheless, our inability to detect dendrimer internalization emphasizes the point that other cell transfection mechanisms have been proposed. For example, the enhanced transfection has been attributed to the dendrimer acting as a proton sponge in the acidic endosomes which leads to osmotic swelling and endosome lysis (*3*). Another possibility is increased resistance to DNA degradation (*29*, *30*). Finally, fractured dendrimers have been reported with enhanced transfection activities, an observation attributed to their more flexible structures (*3*, *8*). It is apparent that further studies are needed to clearly delineate the factors controlling gene delivery using PAMAM dendrimers (*29*, *30*, *51*).

CONCLUSION

We find that high-generation, polycationic PAMAM dendrimers are able to disrupt anionic vesicles much better than low-generation dendrimers or linear poly(lysine). The high-generation dendrimers also have a special ability to induce anionic membranes to adopt inverse curvature. The results are rationalized in terms of a dendrimer-induced membrane bending model. Although the model is somewhat speculative, it does provide a simple physical picture that suggests how polycationic dendrimers may act in various drug delivery and cell transfection applications.

ACKNOWLEDGMENT

We thank Y. Vandenburg for preparing the DNA plasmid samples and Dr. J. Zajicek for assistance with the ^{31}P NMR. This work was supported by the National Institutes of Health (GM 59078).

LITERATURE CITED

(1) Kim, Y., and Zimmerman, S. C. (1998) *Curr. Opin. Chem. Biol. 2*, 733−742.
(2) Tomalia, D. A., and Durst, H. D. (1993) in *Topics in Curr. Chem.* (E. Weber, Ed.) pp 193−313, Springer-Verlag, Berlin.
(3) Tang, M. X., Redemann, C. T., and Szoka, F. C. (1996) *Bioconjugate Chem. 7*, 703−714.
(4) Kukowska-Latallo, J. F., Bielinska, A. U., Johnson, J., Spindler, R., Tomalia, D. A., and Baker, J. R. (1996) *Proc. Natl. Acad. Sci. U.S.A. 93*, 4897−4902.
(5) Goncz, K. K., Kunzelmann, K., Xu, Z. D., and Gruenert, D. C. (1998) *Hum. Mol. Gen. 7*, 1913−1919.
(6) Qin, L. H., Pahud, D. R., Ding, Y. Z., Bielinska, A. U., Kukowska-Latallo, J. F., Baker, J. R., and Bromberg, J. S. (1998) *Hum. Gene Ther. 9*, 553−560.
(7) Alahari, S. K., DeLong, R., Fisher, M. H., Dean, N. M., and Juliano, R. L. (1998) *J. Pharm. Exp. Ther. 286*, 419−428.
(8) Ruponen, M., Yla-Herttuala, S., and Urtti, A. (1999) *Biochim. Biophys. Acta 1415*, 331−341.
(9) Turnen, M. P., Hiltunen, M. O., Ruponen, M., Virkamaki, L., Szoka, F. C., Urtti, A., and Yla-Hertuala, S. (1999) *Gene Ther. 6*, 6−11.
(10) Hudde, T., Rayner, S. A., Comer, R. M., Weber, M., Issacs, J. D., Waldmann, H., Larkin, D. P. F., and George, A. J. T. (1999) *Gene Ther. 6*, 939−943.
(11) Dunphy, E. J., Redman, R. A., Herweijer, H., and Cripe, T. P. (1999) *Hum. Gene Ther. 10*, 2407−2417.
(12) Toth, I., Sakthivel, T., Widerspin, A. F., Bayele, H., O'Donnell, M., Perry, D. J., Pasi, K. J., Lee, C. A., and Florence, A. T. (1999) *S.T.P. Pharma Sci. 9*, 93−99.
(13) Kukowska-Latallo, J. F., Chen, C. L., Eichman, J., Bielinska, A. U., and Baker, J. R. (1999) *Biochem. Biophys. Res. Commun. 264*, 253−261.
(14) Loup, C., Zanta, M., Caminade, A., Majoral, J., and Meunier, B. (1999) *Chem. Eur. J. 5*, 3644−3650.
(15) Jackson, C. J., Chanzy, H. D., Booy, F. P., Drake, B. J., Tomalia, D. A., Bauer, B. J., and Amis, E. J. (1998) *Macromolecules 31*, 6259−6265.
(16) Düzgünes, N, Allen, T. M., Fedor. J., and Paphadjopoulos, D. (1987) *Biochemistry 26*, 8435−8442.
(17) Düzgünes, N., and Wilschut, J. (1993) *Methods Enzymol. 220*, 3−14.
(18) Bondeson, J., and Sundler, R. (1990) *Biochim. Biophys. Acta 1026*, 186−194.
(19) Kendall, D. A., and MacDonald, R. C. (1982) *J. Biol. Chem. 257*, 13892−13898.
(20) Rance, M., and Byrd, A. (1983) *J. Magn. Reson. 52*, 221−240.
(21) Tedesco, M., and Matile, S. (1999) *Bioorg. Med. Chem. 7*, 1373−1379.
(22) Gad, A, Bental, M., Elyahiv, G., and Weinberg, H. (1985) *Biochemistry 24*, 6277−6282.
(23) Walter, A., Steer, C. J., and Blumenthal, R. (1986) *Biochim. Biophys. Acta 861*, 319−330.
(24) Oku, N., Yamaguchi, N., Yamaguchi, N., Shibamoto, S., Ito, F., and Nango, M. (1986) *Biochem. J. 100*, 935−944.
(25) McIntosh, T. J., Kulkarni, K. G., and Simon, S. A. (1999) *Biophys. J. 76*, 2090−2098.
(26) Holland, J. W., Hui, C., Cullis, P. R., and Madden, T. D. (1996) *Biochemistry 35*, 2618−2624.
(27) Düzgünes, N., Nir, S., Wiscut, J., Bentz, J., Newton, C., Portis, A., and Papahadjoloulos, D. (1981) *J. Membr. Biol. 59*, 115−125.
(28) Rolland, A. P. (1998) *Crit. Rev. Ther. Drug Carrier Sys. 15*, 143−198.
(29) Bielinska, A. U., Kukowska-Latallo, J. F., and Baker, J. R. (1997) *Biochim. Biophys. Acta 1353*, 180−190.
(30) Bielinska, A. U., Chen, C. L., Johnson, J., and Baker, J. R. (1999) *Bioconjugate Chem. 10*, 843−850.
(31) Junker, M., and Creutz, C. E. (1993) *Biochemistry 32*, 9968−9974.
(32) Epand, R. M., and Lim, W. (1995) *Biosci. Rep. 15*, 151−160.
(33) Bradley, A. J., Maurer-Spurej, E., Brooks, D. E., and Devine, D. V. (1999) *Biochemistry 38*, 8112−8123.
(34) Yeagle, P. L. (1996) in *Handbook of Nonmedical Applications of Liposomes, Vol. II., Models for Biological Phenomena* (D. D. Lasic and Y. Barenholz, Eds.) Chapter 5, CRC, Boca Raton.
(35) DeKrujiff, B., and Cullis, P. R. (1980) *Biochim. Biophys. Acta 602*, 477−490.
(36) DeKrujiff, B., and Cullis, P. R. (1980) *Biochim. Biophys. Acta 601*, 235−240.
(37) Balch, C., Morris, R., Brooks, E., and Sleight, R. G. (1994) *Chem. Phys. Lipids 70*, 205−212.
(38) Ben-Tal, N., Honig, B., Peitzsch, R. M., Denisov, G., and McLaughlin, S. (1996) *Biophys. J. 71*, 561−575.
(39) Kim, J., Mosior, M., Chung, L. A., Wu, H., and McLaughlin, S. (1991) *Biophys. J. 60*, 135−148.
(40) Gad, A. E., Silver, B., and Eytan, G. D. (1982) *Biochim. Biophys. Acta 690*, 124−132.
(41) Gad, A. E., Bental, M., Elyashiv, M., and Weinberg, H. (1985) *Biochemistry 24*, 6277−6282.
(42) Talbot, W. A., Zheng, L. X., and Lentz, B. R. (1997) *Biochemistry 36*, 5827−5836.
(43) Takahashi, H., Yasue, T., Ohki, K., and Hatta, I. (1996) *Mol. Membr. Biol. 13*, 233−240.
(44) Fukushima, K., Sakamoto, T., Tsuji, J., Kondo, K., and Shimozawa, R. (1994) *Biochim. Biophys. Acta 1191*, 133−140.
(45) Laroche, G., Carrier, D., and Pézolet, M. (1988) *Biochemistry 27*, 6220−6228.
(46) Fukushima, K., Muraoka, Y., Inoue, T., and Shimozawa, R. (1989) *Biophys. Chem. 34*, 83−90.
(47) Fukushima, K., Muraoka, Y., Inoue, T., and Shimozawa, R. (1988) *Biophys. Chem. 30*, 237−244.
(48) Hartmann, W., Galla, H.-J., and Sackmann, E. (1977) *FEBS Lett. 78*, 169−172.
(49) Lentz, B. (1994) *Chem. Phys. Lipids 73*, 91−106.
(50) Leckband, D. E., Helm, C. A., and Israelachvili, J. (1993) *Biochemistry 32*, 1127−1140.
(51) Ottaviani, M. F., Sacchi, B., Turro, N. J., Chen, W., Jockusch, S., and Tomalia, D. A. (1999) *Macromolecules 32*, 2275−2282.
(52) Ottaviani, M. F., Matteini, P., Brustolon, M., Turro, N. J., Jockusch, S., and Tomalia, D. A. (1998) *J. Phys. Chem. B 102*, 6029−6039.
(53) Ottaviani, M. F., Daddi, R., Brustolon, M., Turro, N. J., and Tomalia, D. A. (1999) *Langmuir 15*, 1973−1980.
(54) Ottaviani, M. F., Montalti, F., Romanelli, M., Turro, N. J., and Tomalia, D. A. (1996) *J. Phys. Chem. 100*, 11033−11042.
(55) Watkins, D. M., Sayed-Sweet, Y., Klimash, J. W., Turro, N. J., and Tomalia, D. A. (1997) *Langmuir 13*, 3136−3141.
(56) Jansen, J. F. G. A., Meijer, W. W., and De Babandander-van den Berg, E. M. M. (1995) *J. Am. Chem. Soc. 117*, 4417−4418.
(57) Chernomordik, L. V., and Zimmerberg, J. (1995) *Curr. Opin. Struct. Biol. 5*, 541−547.

(58) Epand, R. M., and Polozov, I. (1996) in *Handbook of Nonmedical Applications of Liposomes, Vol. II., Models for Biological Phenomena* (D. D. Lasic and Y. Barenholz, Eds.) Chapter 7, CRC, Boca Raton.
(59) McIntosh, T. J., Kulkarni, K. G., and Simon, S. A. (1999) *Biophys. J. 76*, 2090−2098.
(60) Siegel, D. P. (1999) *Biophys. J. 76*, 291−313.
(61) Weber, T., Zemelman, B. V., McNew, J. A., Westerman, B., Gmachi, M., Parlati, F., Söllner, T. H., and Rothman, J. E. (1998) *Cell 92*, 759−772.
(62) Koslov, M. M., and Chernomordik, L. V. (1998) *Biophys. J. 75*, 1384−1396.
(63) Markosyan, R., Melikyan, G. B., and Cohen, F. S. (1999) *Biophys. J. 77*, 943−952.
(64) Densiov, G., Wanaski, S., Luan, P., Glaser, M., and McLaughlin, S. (1998) *Biophys. J. 74*, 731−744.
(65) Kleinschmidt, J. H., and Marsh, D. (1997) *Biophys. J. 73*, 2546−2555.
(66) Xu, G. P., Solaiman, F., Zink, M. A., and Hodgson, C. P. (2000) *Cancer Gene Ther.* 7, 53−58.

BC000018Z